

Electronic Supplementary Information (ESI)

Efficient solar light driven H₂ production: A post-synthetic encapsulation of Cu₂O co-catalyst on metal-organic framework (MOF) for boosting the effective charge-carrier separation

Peramaiah Karthik,^a Ekambaram Balaraman,^{b*} and Bernaurdshaw Neppolian^{a*}

^aSRM Research Institute and Department of Chemistry, SRM University, Kattankulathur,
Chennai- 603203, Tamil Nadu, India.

^bOrganic Chemistry Division, CSIR-National Chemical Laboratory (CSIR-NCL), Dr. Homi
Bhabha Road, Pune-411008, India.

*E-mail: *neppolain.b@res.srm.univ.ac.in*, *eb.raman@ncl.res.in*

Content

1. Figure S1.TEM-EDX of $\text{Cu}_2\text{O}/\text{NH}_2\text{-MIL-125(Ti)}$ MOF.
2. Figure S2.X-ray diffraction patterns of $\text{NH}_2\text{-MIL-125(Ti)}$ and $\text{Cu}_2\text{O}/\text{NH}_2\text{-MIL-125(Ti)}$ MOFs.
3. Figure S3. X-ray diffraction patterns of Cu_2O .
4. Figure S4. N_2 adsorption and desorption isotherms of $\text{NH}_2\text{-MIL-125(Ti)}$ and $\text{Cu}_2\text{O}/\text{NH}_2\text{-MIL-125(Ti)}$ MOF.
5. Figure S5.FT-IR spectra of $\text{NH}_2\text{-MIL-125(Ti)}$ and $\text{Cu}_2\text{O}/\text{NH}_2\text{-MIL-125(Ti)}$ MOFs.
6. Figure S6. Survey scan and $\text{Cu}2\text{p}$ spectra of $\text{Cu}_2\text{O}/\text{NH}_2\text{-MIL-125(Ti)}$ MOFs.
7. Figure S7.Photographs of pristine $\text{NH}_2\text{-MIL-125(Ti)}$ MOF and (b) $\text{Cu}_2\text{O}/\text{NH}_2\text{-MIL-125(Ti)}$ MOF.
8. Figure S8.FT-IR spectra of after the photocatalytic H_2 production.
9. Figure S9.TEM image after the photocatalytic H_2 production.
10. Figure S10.TEM-EDX of $\text{Cu}_2\text{O}/\text{NH}_2\text{-MIL-125(Ti)}$ MOF after the photocatalytic reaction.
11. Figure S11.Photocatalytic H_2 production using physical mixture of Cu_2O and $\text{NH}_2\text{-MIL-125 (Ti)}$ MOF.
12. Figure S12.Raman analysis of $\text{NH}_2\text{-MIL-125(Ti)}$ and $\text{Cu}_2\text{O}/\text{NH}_2\text{-MIL-125(Ti)}$ MOFs.
13. Table S1.Elemental composition of $\text{Cu}_2\text{O}/\text{NH}_2\text{-MIL-125(Ti)}$ MOF.

14. Table S2. The BET surface area and pore volume data of pristine NH₂-MIL-125(Ti) and Cu₂O/ NH₂-MIL-125(Ti) MOF.
15. Table S3. Photocatalytic H₂ production comparison with existing MOF based catalysts.
16. Table S4. Elemental composition of Cu₂O/ NH₂-MIL-125(Ti) MOF after the photocatalytic H₂ production.
17. Apparent Quantum Yield (AQY).

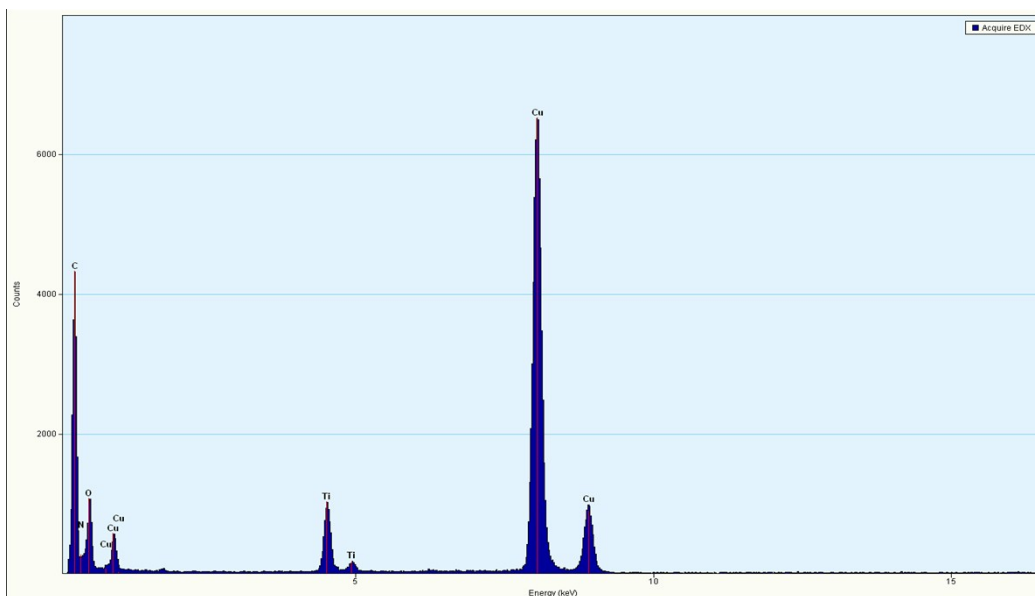


Figure S1. TEM-EDX of $\text{Cu}_2\text{O}/\text{NH}_2\text{-MIL-125(Ti)}$ MOF.

The EDX analysis shows the presence of all the elements such as C, N, O, Ti and Cu in the synthesized Metal-organic framework photocatalyst. The atomic and weight % of elements are tabulated in table S1.

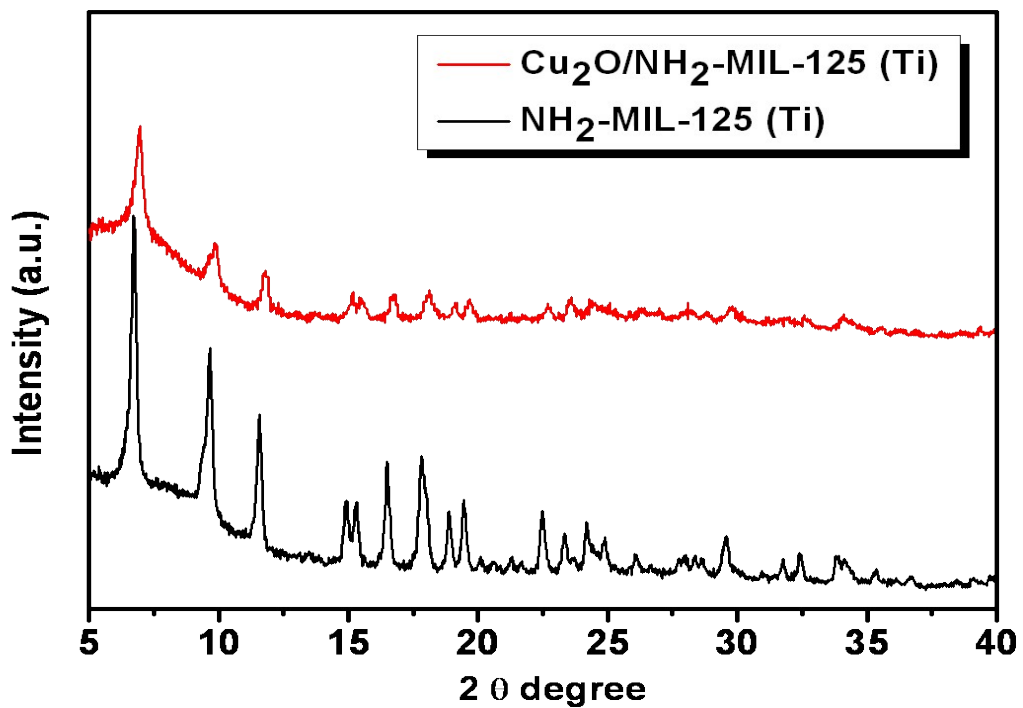


Figure S2. X-ray diffraction patterns of $\text{NH}_2\text{-MIL-125(Ti)}$ and $\text{Cu}_2\text{O}/\text{NH}_2\text{-MIL-125(Ti)}$ MOFs.

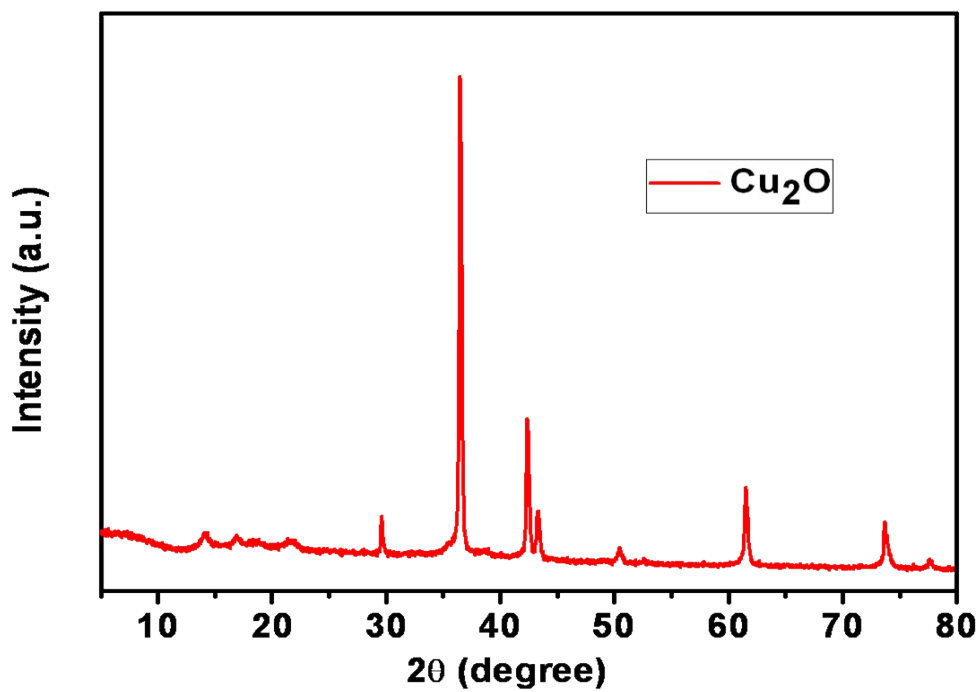


Figure S3. X-ray diffraction patterns of Cu_2O .

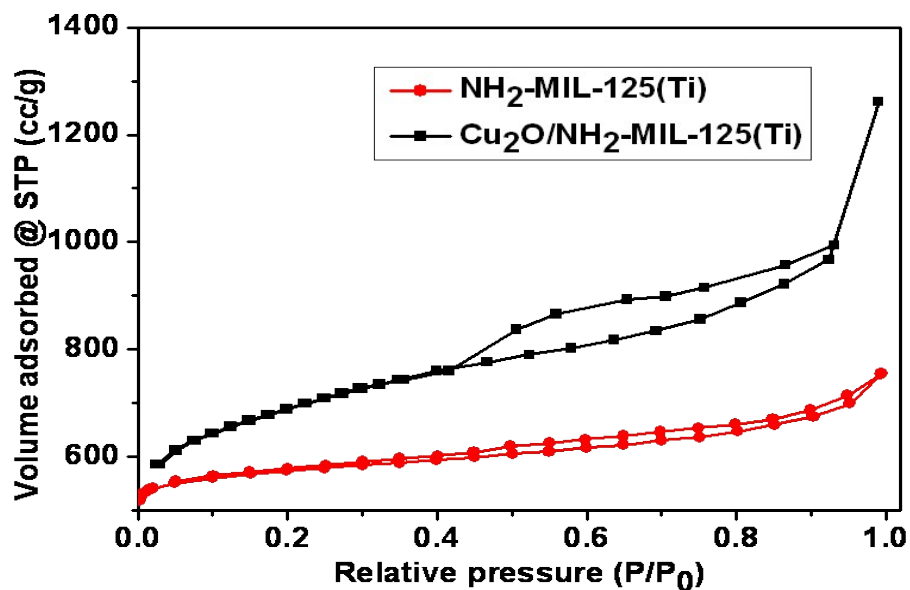


Figure S4. N₂ adsorption and desorption isotherms of NH₂-MIL-125(Ti) and Cu₂O/ NH₂-MIL-125(Ti) MOF.

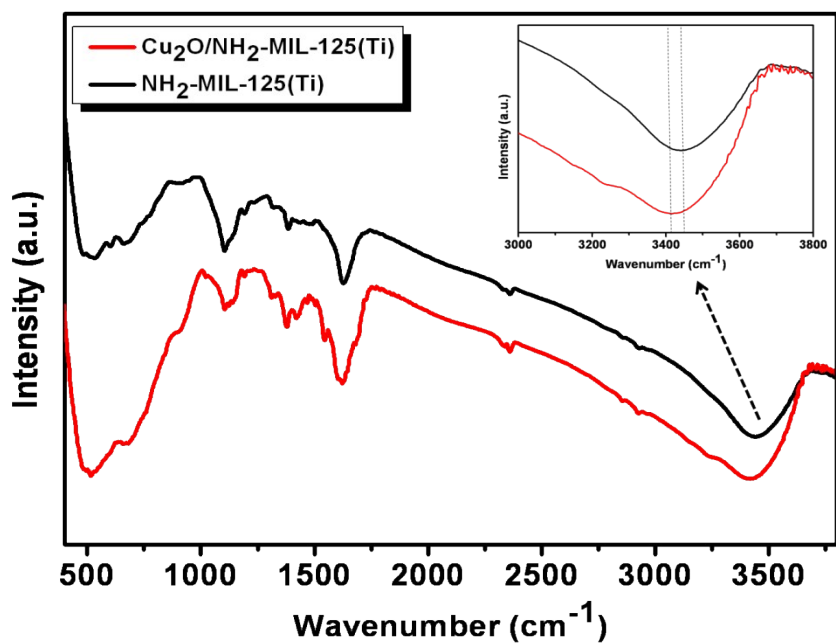


Figure S5. FT-IR spectra of NH₂-MIL-125(Ti) and Cu₂O/ NH₂-MIL-125(Ti) MOFs.

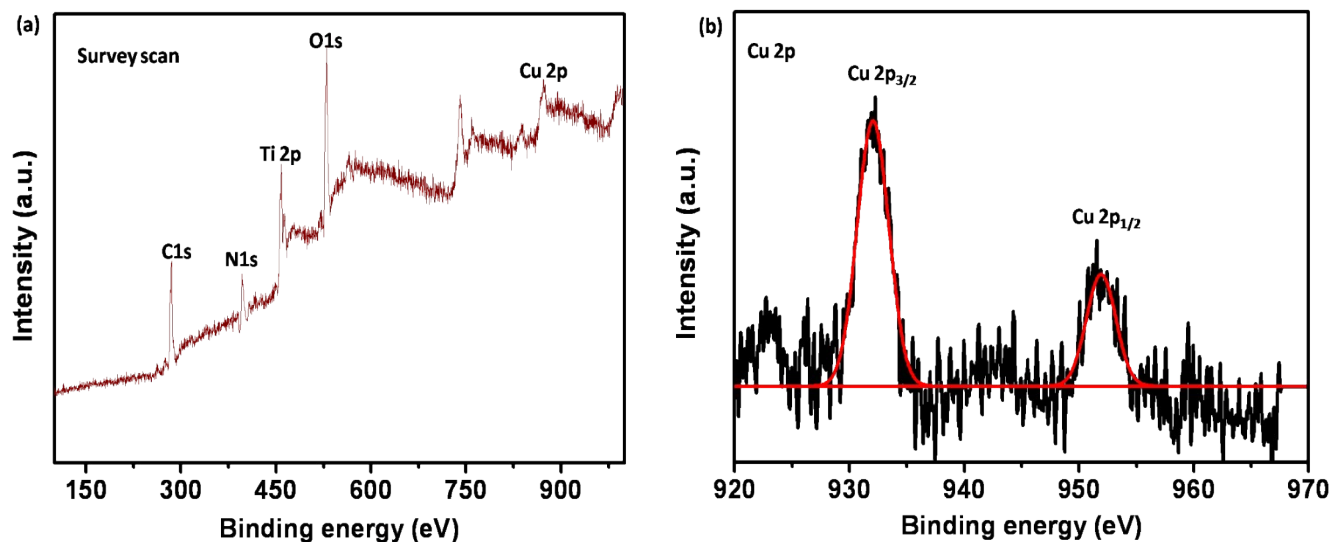


Figure S6. Survey scan and Cu2p spectra of Cu₂O/ NH₂-MIL-125(Ti) MOFs.

The chemical composition and valence states of Cu element were investigated by XPS spectra. The survey scan spectrum (Fig. S5a) clearly reveals the existence of Ti, Cu, O, N and C in the MOF composite. In addition, it is seen from the Cu2p core level spectrum of Cu, the two predominant binding energies such as 932.5 and 952.4 eV was observed related to Cu 2p_{3/2} and Cu 2p_{1/2}, respectively and this obviously demonstrates the formation of Cu₂O.[1] However, the small peak appeared at 945.1 eV due to shake-up of outer electron in the Cu⁺ state.[2]

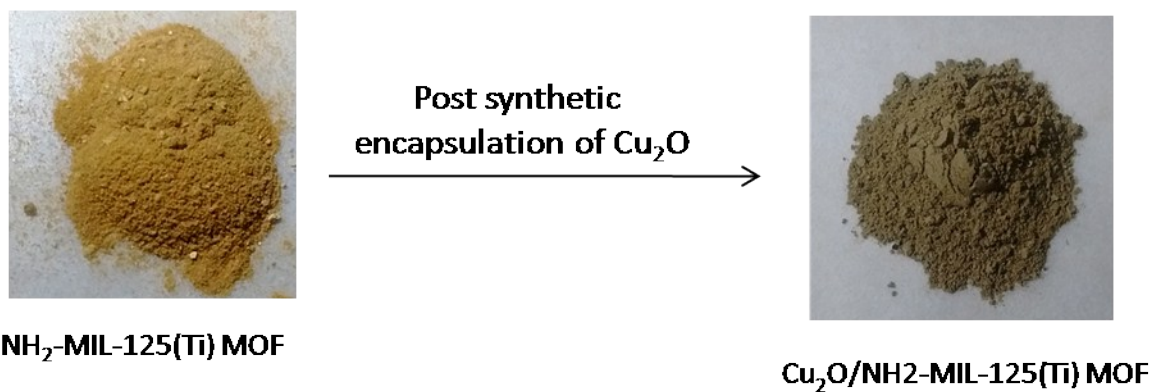


Figure S7. The photographs of pristine NH₂-MIL-125(Ti) MOF and (b) Cu₂O/NH₂-MIL-125(Ti) MOF.

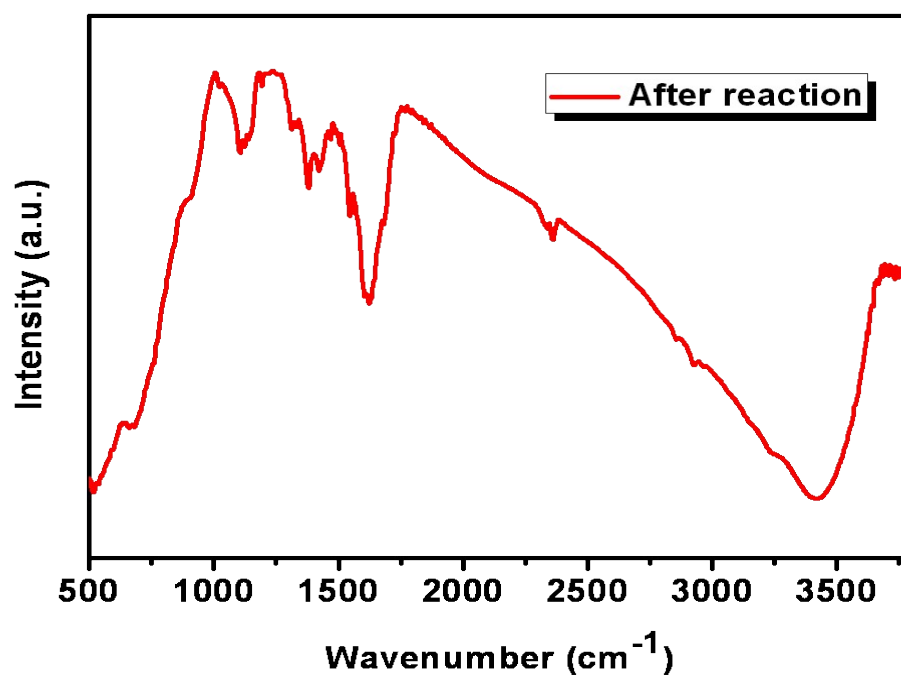


Figure S8. FT-IR spectra of after the photocatalytic H₂ production.

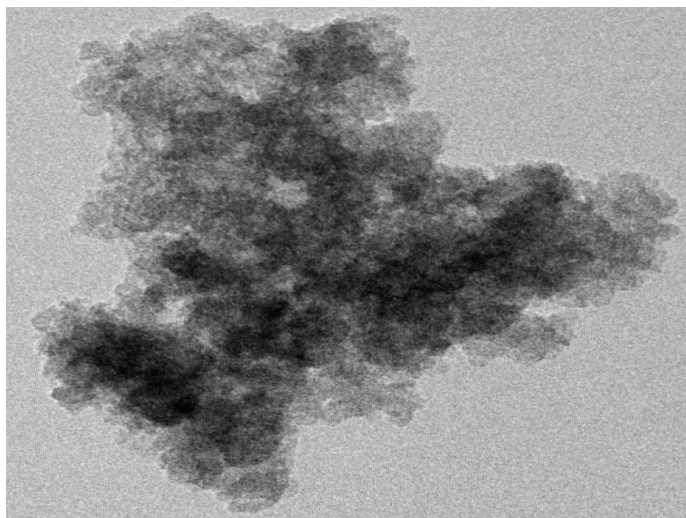


Figure S9. TEM image after the photocatalytic H₂ production.

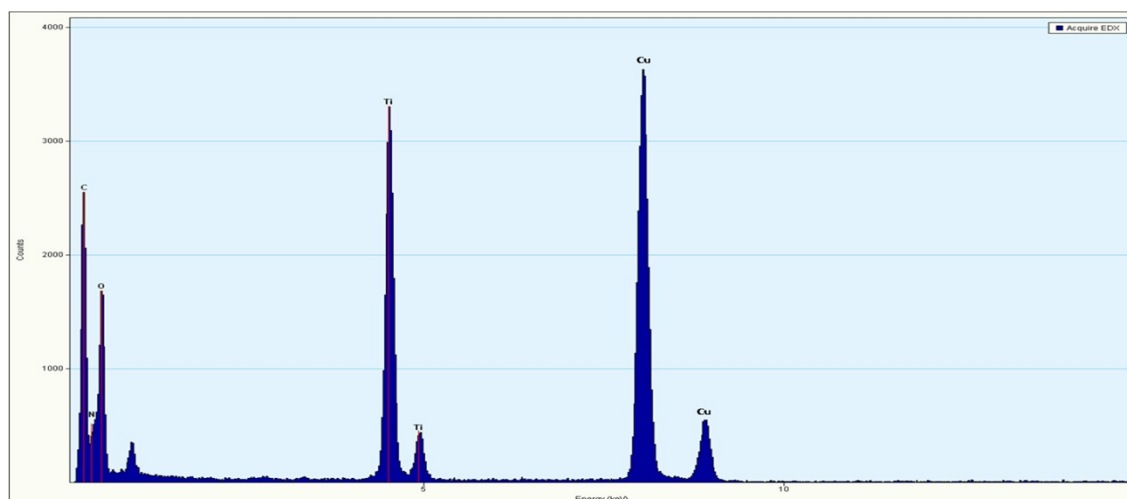


Figure S10. TEM-EDX of Cu₂O/ NH₂-MIL-125(Ti) MOF after the photocatalytic reaction.

The superior stability of Cu₂O/ NH₂-MIL-125(Ti) MOF was further confirmed by the TEM-EDX analysis. It is clearly seen from the Fig. S10 and table S4, there is no significant change in the elemental composition Cu₂O/ NH₂-MIL-125(Ti) MOF after the photocatalytic H₂ production.

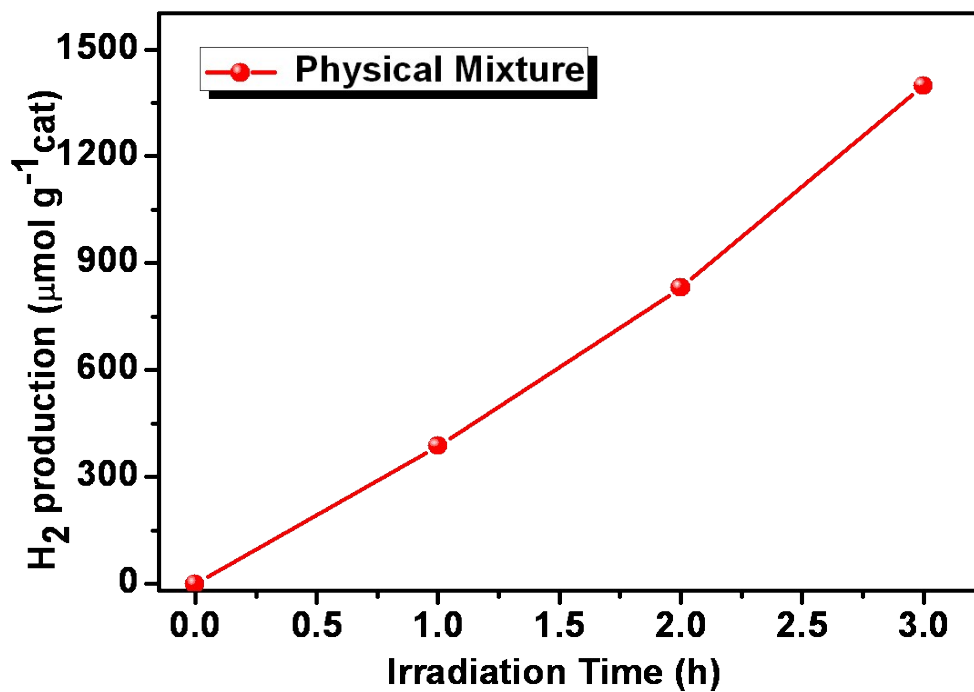


Figure S11. Photocatalytic H₂ production using physical mixture of Cu₂O and NH₂-MIL-125 (Ti) MOF.

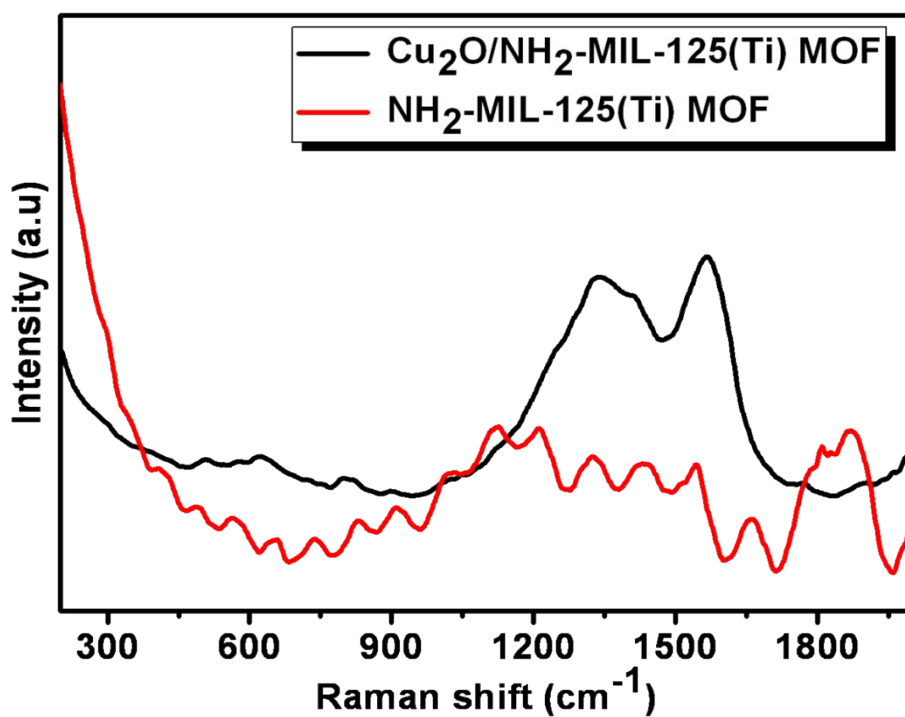


Figure S12. Raman analysis of NH₂-MIL-125(Ti) and Cu₂O/ NH₂-MIL-125(Ti) MOFs.

Table S1. Elemental composition of Cu₂O/ NH₂-MIL-125(Ti) MOF.

Element	Weight %	Atomic %	Uncert. %	Correction	k-Factor
C(K)	37.98	71.18	0.29	0.26	3.94
N(K)	1.25	2.02	0.07	0.26	3.826
N(K)	1.25	2.02	0.07	0.26	3.826
Ti(K)	4.3	2.02	0.05	0.98	1.229
Cu(K)	51.92	18.39	0.21	0.99	1.667

Table S2. The BET surface area and pore volume data of pristine NH₂-MIL-125(Ti) and Cu₂O/ NH₂-MIL-125(Ti) MOF.

Entry	BET surface area (m²/g)	pore volume (nm)
NH ₂ -MIL-125(Ti)	710	0.649
Cu ₂ O/NH ₂ -MIL-125(Ti) MOF	689	0.421

Table S3. Photocatalytic H₂ production comparison with existing MOF based catalysts.

MOF catalyst	Co-catalyst	Reaction conditions	H ₂ evaluation rate	Quantum efficiency	Ref.
MOF-253-Pt	Pt	Light source : 300W Xe Lamp -Visible Sacrificial agent : TEOA	3000 μmol	1.63% at 440 nm	[3]
H ₂ TCPP[Al(OH) ₂](DM F ₃ -(H ₂ O) ₂)	Colloidal Pt	Light source : 300W Xe Lamp -Visible Sacrificial agent : EDTA	200 μmol g ⁻¹ h ⁻¹	0.1 %	[4]
{[Ln ₂ Cu ₅ (OH) ₂ (pydc) ₆ (H ₂ O) ₈]·I8} (Ln: Tb)	-	Light source : 500W Hg Lamp –UV Sacrificial agent : aq. CH ₃ OH	2105 μmol g ⁻¹ h ⁻¹	-----	[5]
RhB/UiO-66(Zr)-100*	Rh-B and Pt	Light source : 300W Xe Lamp –Visible Sacrificial agent : TEOA	116.0 μmol g ⁻¹ h ⁻¹	-----	[6]
Pt-UiO-66-30	Pt	Light source : 300W Xe Lamp -Visible Sacrificial agent : CH ₃ OH	4.6 μmol	~0.25% at 420 nm	[7]
Pt/Ti-MOF-Ru(tpy) ₂	Pt	Light source : 500W Xe Lamp -Visible Sacrificial agent : TEOA	5.1 μmol	-----	[8]
Pt /[Cu(en) ₂] ₄ [PNb ₁₂ O ₄₀ (VO) ₆]·(OH) ₅ ·8H ₂ O	Pt	Light source : 125W Hg Sacrificial agent : aq.CH ₃ OH	44.35 μmol g ⁻¹ h ⁻¹	-----	[9]
Pt@CdS/MIL-101(Cr)	Pt	Light source : 300W Xe Sacrificial agent : lactic acid	150 μmol g ⁻¹ h ⁻¹	-----	[10]
Co@NH ₂ -MIL-125(Ti)	Co	Light source : 500W Xe/Hg Sacrificial agent : TEOA	37 μmol	0.5 % at 400 nm	[11]
Pt/NH ₂ -MIL-125(Ti)	Pt	Light source : Xe lamp Sacrificial agent : TEOA	33 μmol	-----	[12]
Pt/MIL-125(Ti)	Pt	Light source : Xe lamp	38.68 μmol	-----	[13]

		($\lambda=320-780$ nm) Sacrificial agent : TEOA			
{[CuI/CuII 2- (DCTP) ₂]NO ₃ ·1.5DM F} _n	Pt	Light source : 200 W Xe Sacrificial agent : CH ₃ OH	160 $\mu\text{mol h}^{-1}$	2.3% at 420 nm	[14]
[CoII(TPA)Cl][Cl]- MIL-125-NH ₂	Co	Light source : 200 W Xe Sacrificial agent : CH ₃ CN and TEOA	553 $\mu\text{mol g}^{-1}\text{h}^{-1}$	-----	[15]
Pt@UiO-66-NH ₂	Pt	Light source : 200 W Xe lamp Sacrificial agent : CH ₃ CN and TEOA	257.3 $\mu\text{mol g}^{-1} \text{h}^{-1}$	-----	[16]
Cu₂O/ NH₂-MIL- 125(Ti) MOF	Cu₂O	Light source : Solar light Sacrificial agent : 5 %TEOA	11055.5 $\mu\text{mol h}^{-1}\text{g}^{-1}$	1.4 % at 420 nm	This work

Table S4. Elemental composition of Cu₂O/ NH₂-MIL-125(Ti) MOF after the photocatalytic reaction.

Element	Weight %	Atomic %	Uncert. %	Correction	k-Factor
C(K)	35.37	48	0.34	0.26	3.94
N(K)	2.19	2.55	0.11	0.26	3.826
O(K)	43.79	44.61	0.29	0.49	1.974
Ti(K)	0.64	0.21	0.02	0.98	1.229
Cu(K)	17.98	4.61	0.16	0.99	1.667

Apparent Quantum Yield (AQY).

The AQY of photocatalytic H₂ production activity was calculated by using 420 nm band pass filter. The irradiation area was calculated as 0.00144 m²

AQY Calculation details:

The energy of one photon (E_{photon}) with wavelength of λ_{inc} (nm) is calculated using the following equation.

$$E_{\text{photon}} = \frac{hc}{\lambda_{\text{inc}}}$$

Here,

h - Planck's constant (J·s)

c - Speed of light (m s⁻¹)

λ_{inc} - wavelength of the incident monochromatic light (m)

Total energy of the incident light (E_{total}) is can be calculated by following equation:

$$E_{\text{total}} = PSt$$

Where,

P - Power density of the incident monochromatic light (W·m⁻²)

S - Irradiation area (m²)

t- Duration of the incident light exposure (s)

The number of incident photons can be obtained through the following equation

$$\text{Number of incident photons} = \frac{E_{\text{total}}}{E_{\text{photon}}hc} = \frac{PS \lambda_{\text{inct}}}{hc}$$

Quantum yield (Q.Y.) which is widely used to evaluate the performance of photocatalysts for water splitting, is defined by the following equation

$$\text{Q.Y.(\%)} = \frac{\text{Q.Y.(\%)} \text{ Number of reacted electrons}}{\text{Number of incident photons}} \times 100$$

Or

$$\text{A.Q.Y.(\%)} = \frac{2 \text{ (Number of H}_2 \text{ molecules evolved)}}{\text{Number of incident photons}} \times 100$$

References

1. J. Chastain, R. C. King and J. Moulder, *Handbook of X-ray photoelectron spectroscopy: a reference book of standard spectra for identification and interpretation of XPS data*, Physical Electronics Division, Perkin-Elmer Corporation Eden Prairie, Minnesota, 1992.
2. X. Y. Dong, M. Zhang, R. B. Pei, Q. Wang, D. H. Wei, S. Q. Zang, Y. T. Fan and T. C. Mak, *Angew. Chem., Int. Ed.* 2016, **55**, 2073-2077.
3. T. Zhou, Y. Du, A. Borgna, J. Hong, Y. Wang, J. Han, W. Zhang and R. Xu, *Energy Environ. Sci.*, 2013, **6**, 3229-3234.
4. A. Fateeva, P. A. Chater, C. P. Ireland, A. A. Tahir, Y. Z. Khimyak, P. V. Wiper, J. R. Darwent and M. J. Rosseinsky, *Angew. Chem. Int. Ed.*, 2012, **124**, 7558-7562.
5. X.-L. Hu, C.-Y. Sun, C. Qin, X.-L. Wang, H.-N. Wang, E.-L. Zhou, W.-E. Li and Z.-M. Su, *Chem. Commun.*, 2013, **49**, 3564-3566.

6. J. He, J. Wang, Y. Chen, J. Zhang, D. Duan, Y. Wang and Z. Yan, *Chem. Commun.*, 2014, **50**, 7063-7066.
7. Y.-P. Yuan, L.-S. Yin, S.-W. Cao, G.-S. Xu, C.-H. Li and C. Xue, *Appl. Catal. B. Environ.*, 2015, **168**, 572-576.
8. T. Toyao, M. Saito, S. Dohshi, K. Mochizuki, M. Iwata, H. Higashimura, Y. Horiuchi and M. Matsuoka, *Chem. Commun.*, 2014, **50**, 6779-6781.
9. J.-Q. Shen, Y. Zhang, Z.-M. Zhang, Y.-G. Li, Y.-Q. Gao and E.-B. Wang, *Chem. Commun.*, 2014, **50**, 6017-6019.
10. J. He, Z. Yan, J. Wang, J. Xie, L. Jiang, Y. Shi, F. Yuan, F. Yu and Y. Sun, *Chem. Commun.*, 2013, **49**, 6761-6763.
11. M. A. Nasalevich, R. Becker, E. V. Ramos-Fernandez, S. Castellanos, S. L. Veber, M. V. Fedin, F. Kapteijn, J. N. Reek, J. Van Der Vlugt and J. Gascon, *Energy Environ. Sci.*, 2015, **8**, 364-375.
12. Y. Horiuchi, T. Toyao, M. Saito, K. Mochizuki, M. Iwata, H. Higashimura, M. Anpo and M. Matsuoka, *J. Phys. Chem. C*, 2012, **116**, 20848-20853.
13. L. Shen, M. Luo, L. Huang, P. Feng and L. Wu, *Inorg. Chem.* 2015, **54**, 1191-1193.
14. Z. L. Wu, C. H. Wang, B. Zhao, J. Dong, F. Lu, W. H. Wang, W. C. Wang, G. J. Wu, J. Z. Cui and P. Cheng, *Angew. Chem. Int. Ed.*, 2016, **55**, 4938-4942.
15. Z. Li, J.-D. Xiao and H.-L. Jiang, *ACS Catal.*, 2016, **6**, 5359-5365.
16. J. D. Xiao, Q. Shang, Y. Xiong, Q. Zhang, Y. Luo, S. H. Yu and H. L. Jiang, *Angew. Chem. Int. Ed.*, 2016, **55**, 9389-9393.